Hindawi Publishing Corporation
Mathematical Problems in Engineering
Volume 2013, Article ID 890427, 9 pages
http://dx.doi.org/10.1155/2013/890427

Research Article

Cooperative Control of Regenerative Braking and Antilock Braking for a Hybrid Electric Vehicle

Guodong Yin[1,2] and XianJian Jin[1]

[1] *School of Mechanical Engineering, Southeast University, Nanjing 211189, China*
[2] *State Key Laboratory of Mechanical Transmission, Chongqing University, Chongqing 400044, China*

Correspondence should be addressed to Guodong Yin; ygd@seu.edu.cn

Received 10 August 2013; Revised 16 October 2013; Accepted 24 October 2013

Academic Editor: Rongni Yang

A new cooperative braking control strategy (CBCS) is proposed for a parallel hybrid electric vehicle (HEV) with both a regenerative braking system and an antilock braking system (ABS) to achieve improved braking performance and energy regeneration. The braking system of the vehicle is based on a new method of HEV braking torque distribution that makes the antilock braking system work together with the regenerative braking system harmoniously. In the cooperative braking control strategy, a sliding mode controller (SMC) for ABS is designed to maintain the wheel slip within an optimal range by adjusting the hydraulic braking torque continuously; to reduce the chattering in SMC, a boundary-layer method with moderate tuning of a saturation function is also investigated; based on the wheel slip ratio, battery state of charge (SOC), and the motor speed, a fuzzy logic control strategy (FLC) is applied to adjust the regenerative braking torque dynamically. In order to evaluate the performance of the cooperative braking control strategy, the braking system model of a hybrid electric vehicle is built in MATLAB/SIMULINK. It is found from the simulation that the cooperative braking control strategy suggested in this paper provides satisfactory braking performance, passenger comfort, and high regenerative efficiency.

1. Introduction

In the hybrid electric vehicle, regenerative braking takes place by transforming the mechanical energy into electric energy via a generator, the electric energy is stored in the energy storing device such as battery or supercapacitor, and the stored energy is recycled to propel the vehicle via a motor. Energy regeneration during braking is an effective approach to improve vehicle efficiency, especially for vehicles in heavy stop and go traffic [1–3].

Generally, in order to ensure appropriate braking performance and energy regeneration, most HEVs are equipped with both an antilock braking system and a regenerative braking system. As one of the most popular active systems of vehicles, the antilock braking system (ABS) helps the driver to maintain control of the vehicle during emergency braking or braking on a slippery road by preventing wheel lockup; it has dramatically improved vehicle stability during braking. The regenerative braking system works together with the antilock braking system for the following reasons: (a) the regenerative braking torque is not large enough to cover the required braking torque; (b) the regenerative braking cannot be used for many reasons such as a high state of charge (SOC) or high temperature of the battery to increase the battery life. In these cases, the antilock braking system works to supply the required braking torque. Therefore, the cooperative control strategy between the antilock braking system and the regenerative braking system is an important issue to research on HEV.

As for the cooperative control strategy, few investigations have been reported. Present research mainly focuses on two different braking aspects. One is the regeneration efficiency of various types of regenerative braking systems for the electric vehicle (EV) and HEV [4, 5]. Wyczalk suggested a mathematical formulation for the regenerative braking energy by considering the charging and discharging efficiencies and showed that a significant improvement in the regenerative braking could be achieved [6]. Yeo et al. proposed a regenerative braking algorithm with CVT ratio control for a parallel HEV equipped with a CVT; the CVT

ratio is controlled to operate the motor on the most efficient region during regenerative braking; the experiments show that the regenerative braking algorithm offers an improved battery SOC [7]. The optimum control strategy was adopted to improve the regeneration efficiency [8]. The other focus is the emergency braking process. Taking advantage of the quick response and accurate control of the motor torque, researchers worldwide have explored a way to introduce the motor torque into an antilock brake system (ABS) control, expecting a better control effect [9–11]. However, these strategies neglected the cooperative control between the conventional hydraulic braking system and the regenerative braking system, and it is difficult to achieve good braking stability and high regenerative braking efficiency simultaneously. Pu et al. and Peng et al. suggested a combined control algorithm, a logic threshold control strategy to control hydraulic braking torque and a fuzzy logic control strategy to adjust regenerative braking torque [12, 13]. Nevertheless, the magnitude of the regenerative torque varies also depending on the vehicle velocity, and the problem of fluctuating vehicle velocity (variable motor input speeds) has not been addressed in the paper. Because of problems such as nonlinearity in the vehicle-braking dynamics and variations in model parameters over a wide range due to variations in road surface and vehicle conditions, conventional ABS controller cannot achieve satisfactory performance. However, sliding-mode control, which is insensitive to parameter variations and external disturbances and is applicable to nonlinear systems, has become widespread [14, 15]. Therefore, a sliding mode controller (SMC) for ABS is designed; in order to reduce the chattering, a boundary-layer method with moderate tuning of a saturation function is also investigated. Based on the wheel slip ratio, battery state of charge (SOC), and the motor speed, a fuzzy logic control strategy (FLC) is proposed in this paper.

2. System Modeling

Simulation is a crucial step of research and development nowadays. In order to test and verify the cooperative braking control strategy and to evaluate the control effect, simulation is required. To carry out the simulation, appropriate models including those of the vehicle (overall dynamics), the tire, the electric motor, the battery, and the hydraulic system were built.

2.1. Vehicle Dynamics. Since only a straight-line braking maneuver is considered, the vehicle model takes into account only longitudinal movement. For a straight-line braking motion, that is, the movement does not include lateral and vertical motions, and the effect of the slight vibration of suspension system, yaw movement can be neglected, as the effect is very small. Therefore, a typical three degrees of freedom vehicle dynamic model, which possesses the fundamental characteristics of an actual system and sufficient accuracy, is used in this paper. These 3-DOF include the longitudinal velocity, the front-wheel angular speed, and the rear-wheel angular speed of the vehicle. In the hybrid electric vehicle, the regenerative braking torque works often only on the front axle of the vehicle; considering this and the normal force transfers, by making use of Newton's second law and law of rotation, the vehicle dynamic model is built; the dynamic equations are therefore derived as follows:

$$\begin{aligned} m\dot{v} &= F_x - F_a - F_f \\ &= \mu_F(\lambda) F_{zF} + \mu_R(\lambda) F_{zR} - F_a - fmg, \end{aligned} \tag{1}$$

$$\begin{aligned} I_\omega \dot{\omega}_F &= F_{xF} R - T_{hF} - T_{fF} - T_m \\ &= \mu_F(\lambda) F_{zF} R - T_{hF} - T_{fF} - T_m, \end{aligned} \tag{2}$$

$$\begin{aligned} I_\omega \dot{\omega}_R &= F_{xR} R - T_{hR} - T_{fR} \\ &= \mu_R(\lambda) F_{zR} R - T_{hR} - T_{fR}, \end{aligned} \tag{3}$$

$$F_{zF} = \frac{mg}{L}\left(l_R + \frac{\dot{v}}{g} h_g\right), \tag{4}$$

$$F_{zR} = \frac{mg}{L}\left(l_F - \frac{\dot{v}}{g} h_g\right), \tag{5}$$

where m, v, F_x, F_a, F_f, and f are the vehicle mass, the longitudinal velocity of the vehicle, the longitudinal force, the air resistance, the rolling resistance, and the coefficient of the rolling resistance, respectively; F_{zF} and F_{zR} are the front tire normal force and the rear tire normal force, respectively. Also, $\mu_F(\lambda)$ and $\mu_R(\lambda)$ are the friction coefficients of the front and rear tires, respectively, and will be described later ((6) and (7)); the friction coefficient is a nonlinear function of some physical variables, including the velocity of the vehicle and wheel slip. I_ω, F_{xF}, and F_{xR} are the inertia moment of the wheel, the longitudinal tire force on the front wheel, and the longitudinal tire force on the rear wheel, respectively; T_{hF}, T_{hR}, T_{fF}, T_{fR}, and T_m are the hydraulic braking torque on the front wheel, the hydraulic braking torque on the rear wheel, the rolling resistance torque on the front wheel, the rolling resistance torque on the rear wheel, and the regenerative braking torque on the front wheel, respectively; l_F is the distance from vehicle center of gravity to front axle center line, l_R is the distance from vehicle center of gravity to rear axle center line, L is the wheel base, and h_g is the height of the center of gravity.

2.2. The Tire. The tire model is a very essential part in vehicle simulation research. The Pacejka nonlinear tire model "Magic Formula" is a widely used tire model in automotive industry, which possesses a high fitting accuracy and was first proposed by Pacejka in 1991. In this paper, Pacejka's nonlinear tire model "Magic Formula" is used. In the tire model of the mathematical descriptions, a set of trigonometric formulas is used to describe the mathematical relation of the athletic parameters of tire. The magic formula tire model is presented by

$$\mu_i(\lambda) = \theta D \sin\left(C \tan^{-1}\left\{B\lambda_i - E\left[B\lambda_i - \tan^{-1}(B\lambda_i)\right]\right\}\right), \tag{6}$$

$$\lambda_i = \frac{v - \omega_i R}{v}, \tag{7}$$

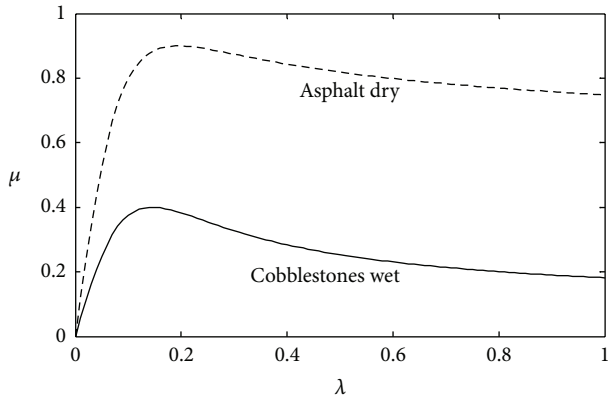

Figure 1: Slip and the friction coefficient relationship based on Pacejka's nonlinear tire model.

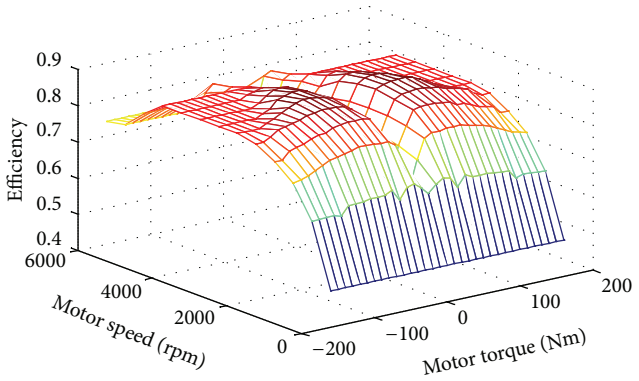

Figure 2: Efficiency characteristics of the electric motor.

where the friction coefficient μ is related to the longitudinal slip ratio λ, i is the rear wheel or the front wheel, and θ is the (maximum) TRFC which has been widely explored and estimated in recent decades. The meanings of the parameters B, C, D, and E can be easily found in the paper by Pacejka and Bakker [16]. Tire models with both high μ and low μ are shown in Figure 1.

2.3. Electric Motor. The motor is used for tractive effort when the battery is discharged and is used as a generator when the battery is charged, in other words in the regenerative braking mode. Based on the test date, an experimental motor model of the mathematical descriptions of the 20 kW PMSM motor is used in this paper, which emphasizes the mathematical relation between inputs and outputs and neglects the complicated physical and electrodynamic movements in electricmotor. The efficiency and torque characteristics of the electric motor are shown in Figure 2.

2.4. The Battery. An experimental battery model of the mathematical descriptions is built, which focuses on the mathematical relation between the charge resistance and the state of charge (SOC). The original capacity of Ni-MH battery is 80 Ah and the nominal voltage is 336 V. In the charging

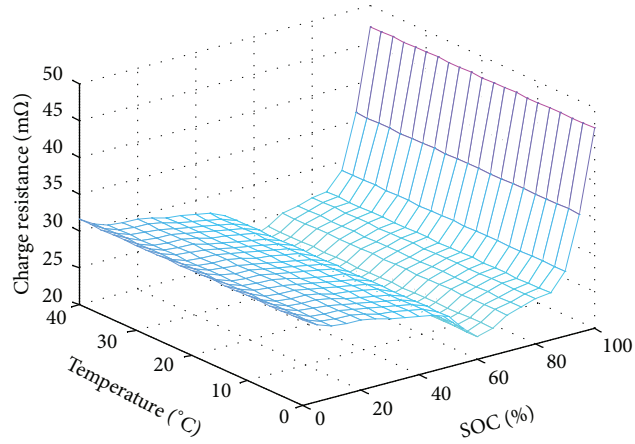

Figure 3: Charging resistance characteristics of the Ni-MH battery.

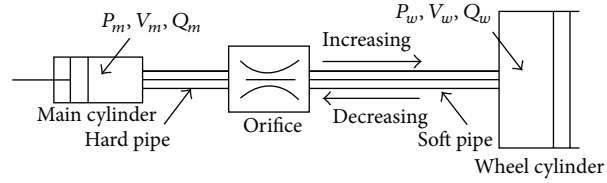

Figure 4: Increasing and decreasing pressure theory diagram of the ABS hydraulic braking system.

or discharging process, the inner resistance of the battery changes depending on the battery's SOC. The characteristics of SOC and the charging resistance of the battery being tested are shown in Figure 3. In the simulation, look-up tables are compiled on the basis of SOC and temperature of the battery, producing its charging-discharging internal resistance.

2.5. Hydraulic System. According to the theory of hydrokinetics and lab tests, the ABS hydraulic system model is described as pressure increasing, pressure holding, and pressure dumping processes, which also uses the mathematical descriptions and neglects the complicated physical process and movement. The theory diagram of the hydraulic pressure increase/decrease is shown in Figure 4. In this paper, the hydraulic system is described by the following equation [17]:

$$\frac{dp_{wi}}{dt} = \begin{cases} 37.54164\left(p_m - p_{wi}\right)^{0.59} & \text{pressure increasing} \\ 0 & \text{pressure holding} \\ -38.3128\left(p_{wi} - p_m\right)^{0.93} & \text{pressure decreasing,} \end{cases} \tag{8}$$

where p_{wi} and p_m are the wheel cylinder pressure and main cylinder pressure, respectively.

3. Cooperative Braking Control Strategy (CBCS) for Regenerative Braking and Antilock Braking

For hybrid electric vehicles, under the effect of regenerative braking torque and hydraulic braking torques, the braking

control system must make the two braking torques work together harmoniously to assure the braking safety of vehicle and maintain comfortable sense for driver. In this paper, the cooperative braking control strategy is divided into two parts: the first part is used to adjust the antilock braking torque in the conventional hydraulic braking system using a sliding mode controller that is based on the target slip ratio to control the braking pressure increase, holding, and decrease; the second part is used to adjust the regenerative braking torque from the electric motor using a fuzzy logic control strategy that is based on the target slip ratio, battery state of charge (SOC), and the motor speed to adjust the regenerative braking torque dynamically. In the cooperative braking control strategy, the wheel slip ratio is the control common variable; the regenerative braking torque and the hydraulic braking toque should be adjusted (increased or decreased) harmoniously based on the changes of slip ratio to assure the braking stability of vehicle.

In the control strategy, the required braking torque of driver T_r can be expressed as

$$T_r = T_h + \beta \cdot T_{mm}, \tag{9}$$

where T_h, β, and T_{mm} are the hydraulic braking torque, the maximum regenerative braking torque which can be added by electric motor at that moment (due to the motor speed), and the load signal of motor, respectively.

3.1. Sliding Mode Controller (SMC). The design procedure of sliding mode control methodology consists of two main steps: first, a sliding surface that models the desired closed-loop performance is chosen, and then, the control law, such that the system state trajectories are forced toward the sliding surface, is derived [18]. Once the sliding surface is reached, the system state trajectories should stay on it. In this paper, SMC is used to track the target slip ratio. Hence, the switching function s is defined as

$$s = \lambda - \lambda_r, \tag{10}$$

where λ_r is the target wheel slip. The sliding motion occurs when the state $(\lambda_r, \dot{\lambda}_r)$ reaches the switching subspace (a point in this case) defined by $s = 0$. The control that keeps the state on the switching subspace is called the equivalent control. In this paper, it is called equivalent control hydraulic braking torque $T_{h-\mathrm{eq}}$. The dynamics in sliding mode can be written as

$$s = 0, \qquad \dot{s} = 0. \tag{11}$$

If it is assumed that the λ_r (the target wheel slip) is constant, substituting (10) into (11) gives

$$\dot{s} = \dot{\lambda} = 0. \tag{12}$$

Differentiation of (7) with respect to time and the use of (1)–(3) gives

$$\begin{aligned}\dot{\lambda} &= \frac{1}{v}\left[-\frac{R}{I}\left(F_x R - T_h - T_f - T_m\right) + (1-\lambda)\,\dot{v}\right] \\ &= -\frac{R}{Iv}\left[\left(F_x R - T_f - T_m\right) - \frac{I}{R}(1-\lambda)\,\dot{v}\right] + \frac{R}{Iv}T_h \\ &= F_p(\lambda, t) + G_p(t)\,u(t),\end{aligned} \tag{13}$$

where $F_p(\lambda, t) = -(R/Iv)[(F_x R - T_f - T_m) - (I/R)(1-\lambda)\dot{v}]$, $G_p(t) = (R/Iv)$, and $u(t) = T_h$ is the control law, assume that the parameters of the system are well known, and rewriting (13), it can represent the nominal model as

$$\dot{\lambda} = F_0(\lambda, t) + G_0(t)\,u(t), \tag{14}$$

where $F_0(\lambda, t)$ and $G_0(t)$ are the nominal values of $F_p(\lambda, t)$ and $G_p(t)$, respectively. If the uncertainties occur, then the controlled system can be modified as

$$\begin{aligned}\dot{\lambda} &= \left[F_0(\lambda, t) + \Delta F(\lambda, t)\right] + \left[G_0(t) + \Delta G(t)\right]u(t) \\ &= F_0(\lambda, t) + G_0(t)\,u(t) + W,\end{aligned} \tag{15}$$

where $\Delta F(\lambda, t)$ and $\Delta G(t)$ denote the system uncertainties and W is referred to as the lump uncertainty and is defined as $W = \Delta F(\lambda, t) + \Delta G(t)u(t)$ with the assumption $|W| \le k$, in which k is a positive constant of the uncertainty bound and will be chosen and described later in (20) and (21).

Substituting (13) into (12) gives

$$T_{h-\mathrm{eq}} = F_x R - T_f - T_m + (1-\lambda)\frac{I}{R}\dot{v}. \tag{16}$$

If the system state $(\lambda_r, \dot{\lambda}_r)$ is not on the switching subspace, an additional control term called hitting control brake torque should be added to the overall brake torque control signals. When the system state is on the switching subspace, the hitting control is zero. The hitting control is assumed to have the form

$$T_{h-h} = k \cdot \mathrm{sgn}(s). \tag{17}$$

The hitting control brake torque is determined by the following reaching condition, where η is a strictly positive design parameter:

$$s\dot{s} \le -\eta\,|s|. \tag{18}$$

Using (10) and (13), (18) can be rewritten as

$$s\dot{\lambda} \le -\eta\,|s|. \tag{19}$$

Substitution of (13) into (19) results in

$$\begin{aligned}&-\frac{sR}{vI}\left[F_x R - T_f - T_m - \left(T_{h-\mathrm{eq}} - k \cdot \mathrm{sgn}(s)\right)\right] \\ &\quad + \frac{s(1-\lambda)\,\dot{v}}{v} \le -\eta\,|s|.\end{aligned} \tag{20}$$

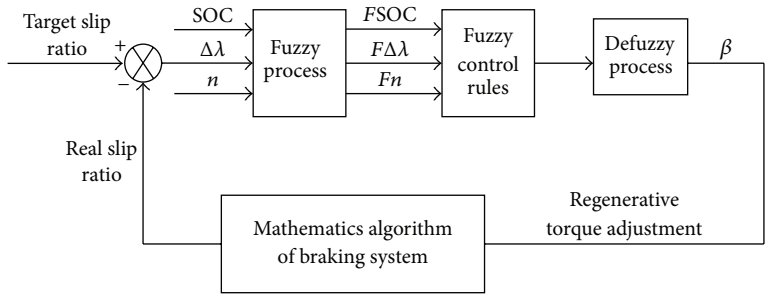

Figure 5: Block diagram of the fuzzy logic controller for the regenerative braking system.

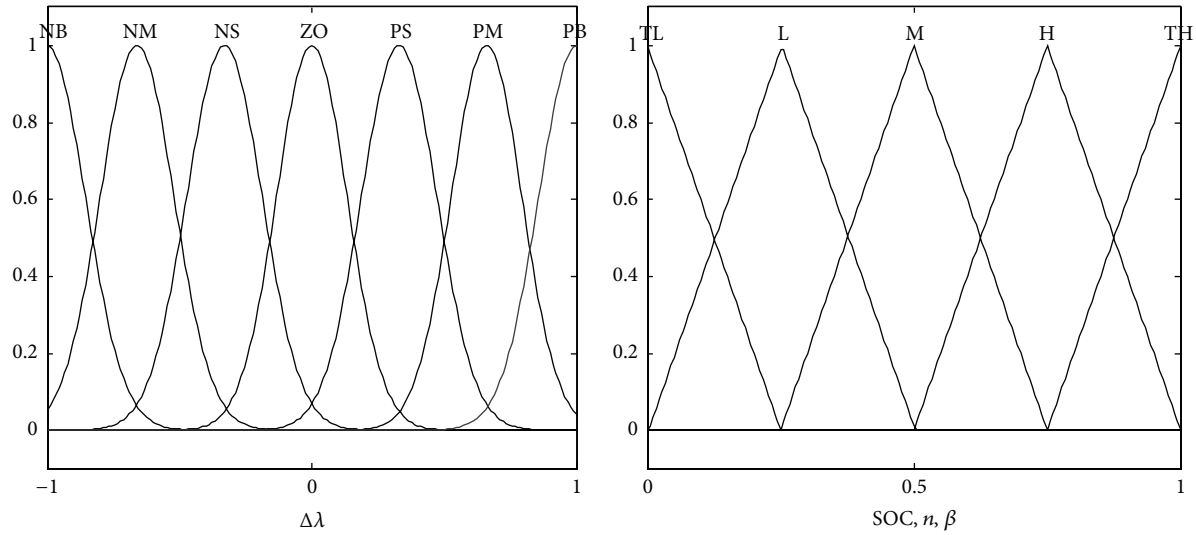

Figure 6: Membership functions for the inputs and outputs of the fuzzy logic controller.

Solving for the switching control gain, the following inequality is obtained:

$$k \geq \frac{vI}{R}\eta. \tag{21}$$

The equation can guarantee that the system is asymptotically stabilized via the switching surface and compensate uncertainties in the simulation model. Chattering phenomenon is an undesirable effect of discontinuous control command during sliding mode control. To reduce the chattering phenomena, a boundary-layer method with moderate tuning of a saturation function is used. The sign function is replaced by saturation function, and the overall hydraulic braking torque control can be rewritten as

$$\begin{aligned} T_h &= T_{h-\mathrm{eq}} + T_{h-h} = F_x R - T_f - T_m \\ &\quad + (1-\lambda)\frac{I}{R}\dot{v} + k \cdot \mathrm{sgn}\left(\frac{s}{\varphi}\right), \end{aligned} \tag{22}$$

where φ is the boundary layer.

3.2. Fuzzy Logic Control Strategy (FLC). A fuzzy logic control strategy is used to adjust the regenerative braking torque dynamically. There are three inputs in the fuzzy logic controller and the three inputs are the difference ($\Delta\lambda$) between the real slip ratio and the target slip ratio, the state of charge (SOC) of the battery, and the motor rotation speed n, respectively. The output is the load signal of electric motor β. The fuzzy logic controller of the regenerative braking system is shown in Figure 5.

Based on the simulation analysis, the $\Delta\lambda$ is divided into six fuzzy subsets: [NB, NM, NS, ZO, PS, PM, PB], where NB, NM, NS, ZO, PS, PM, and PB are negative big, negative medium, negative small, zero, positive small, positive medium, and positive big, respectively. Similarly, the SOC, n, and β are divided into five fuzzy subsets: [TL, L, M, H, TH], where TL, L, M, H, and TH are too low, low, medium, high, and too high, respectively. Gaussian and triangular shapes (as shown in Figure 6) are selected for the membership functions of the inputs and outputs.

Assuming that there are m rules in a fuzzy rule base and each of them has the following form:

$$\begin{aligned} &\text{Rule } i\text{: If } \Delta\lambda \text{ is } S_i \text{ and } SOC \text{ is } P_i \text{ and } n \text{ is } Q_i, \\ &\qquad \text{then } \beta \text{ is } \alpha_i, \end{aligned} \tag{23}$$

Table 1: Vehicle parameters.

PMSM	Power M/G	20/13 KW
Battery	Capacity	80 Ah
	Nominal voltage	336 V
Vehicle	Vehicle mass m	1320 kg
	Tire radius R	0.272 m
	I_ω	1.1 kg·m^2
	f	0.015
	B, C, D, E of tire	8.9, 1.6, 1, 0.5
	L, h_g, l_F, l_R	2.4, 0.5, 0.9, 1.4 (m)
	CVT gear ratio	0.451~2.462

where S_i, P_i, and Q_i are fuzzy subsets and α_i are the singleton control actions for $i = 1, 2, 3, \ldots, m$, the defuzzification of the fuzzy logic controller output is accomplished by the method of center-of-gravity:

$$\beta = \sum_{i=1}^{m} \omega_i \times \alpha_i \sum_{i=1}^{m} \omega_i, \tag{24}$$

where ω_i is the firing weight of the ith rule. Equation (24) can be rewritten as

$$\beta = \alpha^T \xi, \tag{25}$$

where $\alpha = [\alpha_1, \alpha_2, \ldots, \alpha_m]^T$ is a parameter vector and $\xi = [\xi_1, \xi_2, \ldots, \xi_m]^T$ is a regressive vector with ξ_i defined as

$$\xi_i = \frac{\omega_i}{\sum_{i=1}^{m} \omega_i}. \tag{26}$$

Figure 7 presents the output surface of the fuzzy inference regenerative braking system. The Mamdani method is used to perform the fuzzy logic calculation in this paper.

4. Simulation and Analysis

In order to evaluate the performance of the cooperative braking control strategy, the simulation is implemented in MATLAB/SIMULINK. The simulation parameters of main components of the vehicle are listed in Table 1. In Table 1, these values of f, B, C, D, and E are selected from engineers' experiences and tests; values of the other parameters based on a typical car of our laboratory are selected. The simulation includes two parts: one part checks the brake stability during emergency braking, and the other part checks the regenerative efficiency under the New European Driving Cycle (NEDC).

4.1. Simulation for Emergency Braking. First, the vehicle was brought to a steady longitudinal velocity of 30 m/s along a straight path. Then, the ABS and the regenerative braking were applied on the front wheels simultaneously. To increase stability and manoeuvrability of the vehicle and to decrease the stopping distance during emergency braking, the CBCS is implemented to maintain the target slip ratio value of 0.2. The simulation results are shown in Figures 8 and 9.

The wheel speed and slip ratio with conventional control and SMC control are compared in Figures 8(a) and 8(b), respectively. As can be seen in Figures 8(a) and 8(b), the conventional controller and SMC try to stop the car quickly and keep the slip ratio at the optimal value of 0.2; the initial action of the SMC ABS is similar to conventional braking until the sliding surface is reached, and then there is a sharp fall in the wheel speed for SMC, which is due to the hitting control; large oscillations can be observed in the conventional controller; it may be significantly affected by changes in the parameters. The oscillation when using the SMC is much smaller than that when using the conventional controller; perhaps the SMC has more robustness against parameter variation. The sliding mode ABS control produces smoother variations in wheel speed and the slip ratio as compared to the conventional ABS system, thereby improving braking stability and passenger comfort. It can be seen that the wheels are never locked during the whole braking process and the time taken for stopping the car is less than 0.2 s when emergency braking with SMC ABS is used as compared to emergency braking with conventional ABS. Hence, the control performance of the proposed SMC is far better than that of the conventional controller.

Figures 9(a) and 9(b) show the variations in the braking torque and battery SOC in an emergency braking condition. The variations of the hydraulic braking torque and regenerative braking torque are shown in Figure 9(a). Initially, to increase braking stability and manoeuvrability of the vehicle, the hydraulic braking torque is much larger than the regenerative braking torque, and then in order to get more regenerative energy, the cooperative control strategy depresses the hydraulic braking torque of the front axle and increases the regenerative braking toque at the same time. The hydraulic braking torque and regenerative braking torque can cooperate well under the braking control strategy. In Figure 9(b), the battery SOC shows an increased value of about 1.6 percent during emergency braking. Note that if the original battery SOC is small, then braking from the same initial speed to complete rest produces more change in the battery SOC as compared to the case when the battery is initially at a higher SOC. For very large battery SOC, no further charging may be possible and regenerative braking fails.

4.2. Simulation for the NEDC. Simulation results are shown in Figure 10. Figure 10(a) shows the vehicle speed of the New European Driving Cycle (NEDC). Figure 10(b) shows the variations of the hydraulic braking torque and regenerative braking torque. As shown in Figure 10(b), in normal braking process, the electric motor acts as the main braking source, and the hydraulic braking system works only to ensure the parking; in an emergency braking condition, to increase braking stability, the hydraulic braking system acts as the main braking source. The battery current (Figure 10(c)) shows a positive value when the battery is charged and shows a negative value when the battery is discharged. The battery SOC (Figure 10(d)) decreases when the motor is used to propel the vehicle and increases when the motor is used as a generator. The final battery SOC by the FLC control is

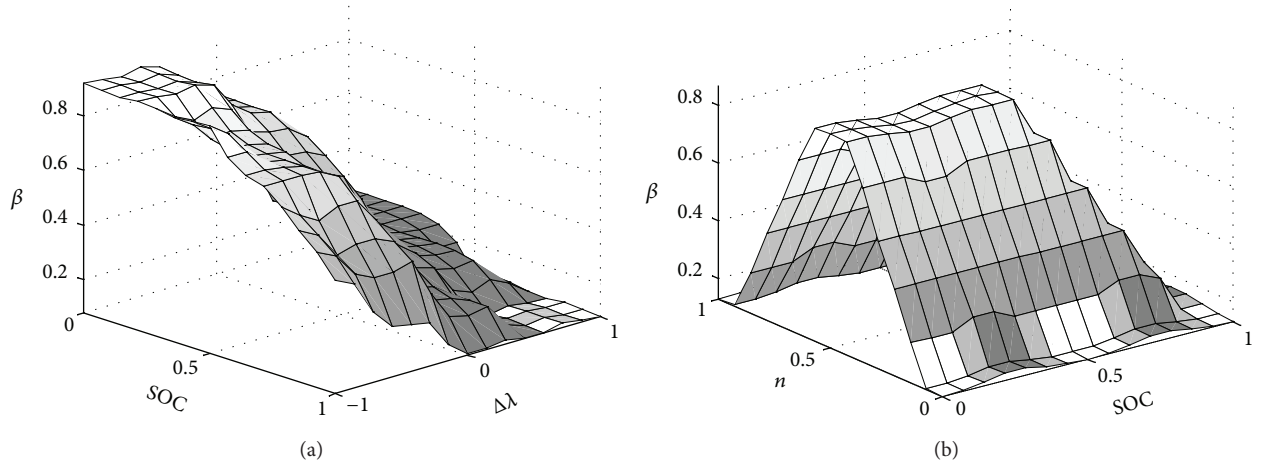

FIGURE 7: Output surface of the fuzzy inference regenerative braking system.

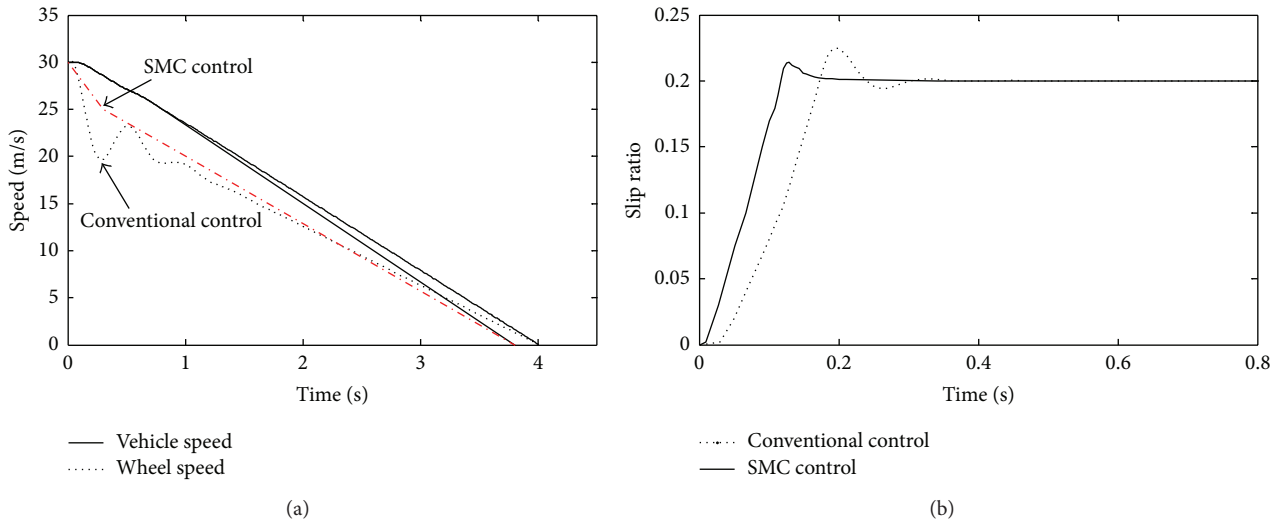

FIGURE 8: Comparison of (a) vehicle speed and wheel speed and (b) slip ratio for conventional control and SMC control.

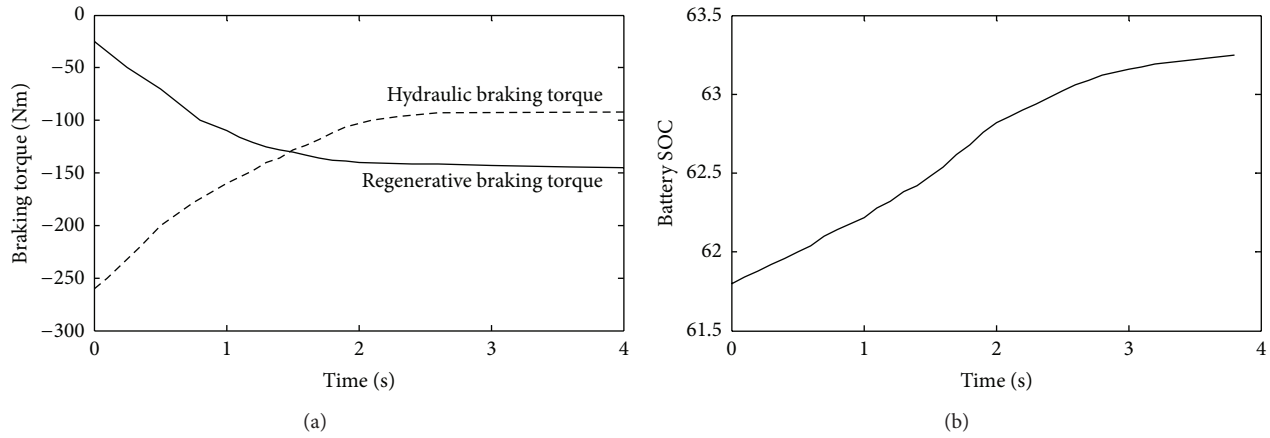

FIGURE 9: (a) Regenerative braking torque and hydraulic braking torque and (b) battery SOC for CBCS during emergency braking by ABS and regenerative braking.

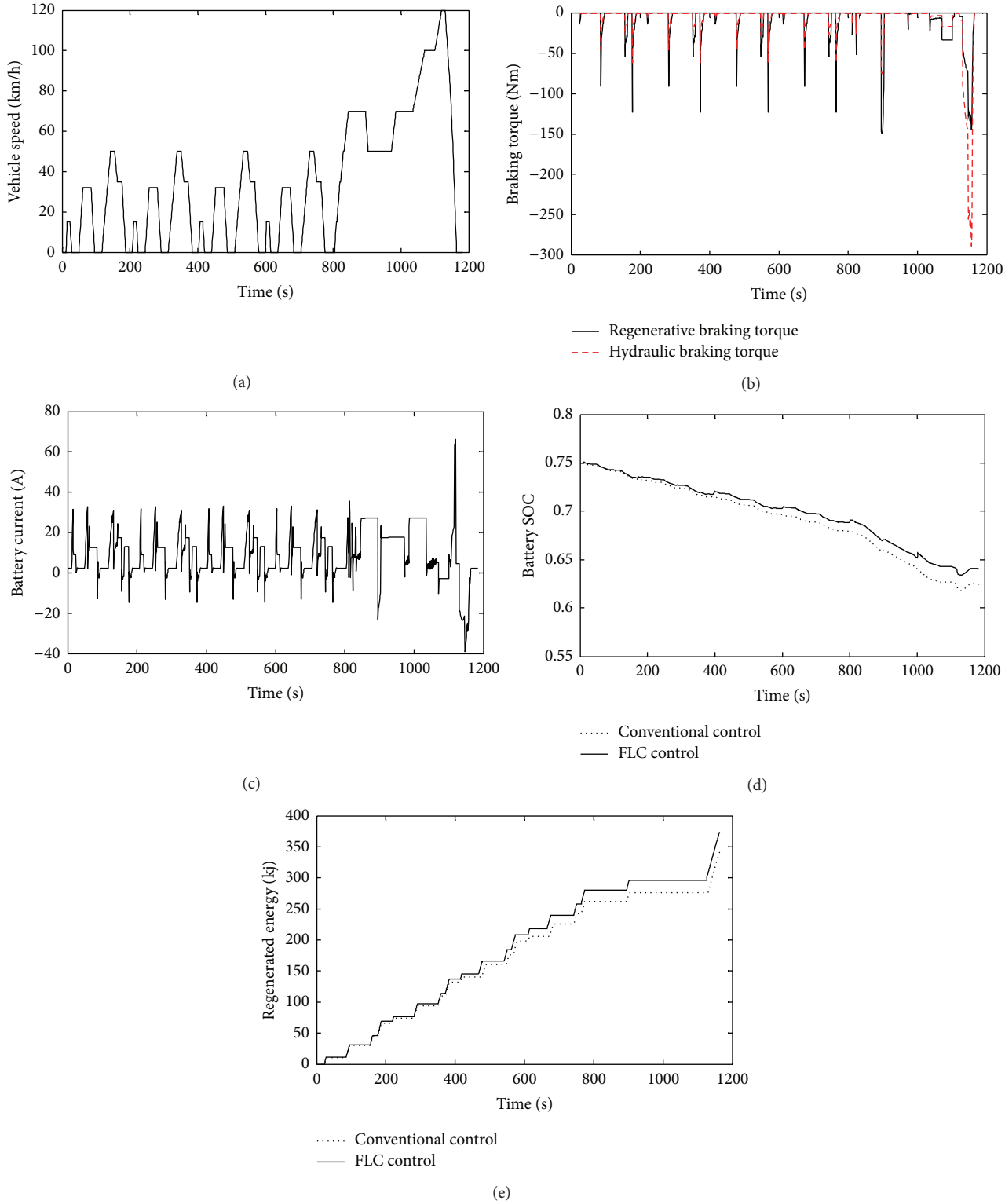

Figure 10: Simulation results for the NEDC.

higher than that by the conventional control, which implies that more electric energy is stored by the FCS control. In Figure 10(e), the regenerated energy stored in battery is compared. As shown in Figure 10(e), the stored energy by the FCS control shows a higher value than that by the conventional control. Since the stored energy can be reused to propel the vehicle, the vehicle fuel economy can be improved by the amount of increased stored energy.

5. Conclusion

A new cooperative braking control strategy (CBCS) for a parallel hybrid electric vehicle is proposed in this paper. The CBCS combines a sliding mode controller and a fuzzy logic control strategy to ensure the vehicle's longitudinal braking performance, which keeps the wheels from being locked and regenerates more energy effectively. The simulation shows that the model of the HEV's braking system and the cooperative braking control strategy developed in this paper are right. It is also found from the simulation that the cooperative braking control strategy suggested in this paper provides satisfactory braking performance, passenger comfort, and high regenerative efficiency. Although the simulation results have a certain guiding significance for real applications, the deviation between the simulation model and the braking system of actual vehicle is inevitable. Hence, the real vehicle test and a hardware-in-the-loop simulation with cosimulations between MATLAB/SIMULINK and dSPACE will be researched to validate the effectiveness of the proposed cooperative braking control strategy in the future.

Acknowledgments

The paper is supported by NSFC (no. 51105074) and Foundation of State Key Laboratory of Mechanical Transmission (SKLMT-KFKT-201206).

References

[1] C. Park, K. Kook, K. Oh, D. Kim, and H. Kim, "Operation algorithms for a fuel cell hybrid electric vehicle," *International Journal of Automotive Technology*, vol. 6, no. 4, pp. 429–436, 2005.

[2] H. Yeo and H. Kim, "Hardware-in-the-loop simulation of regenerative braking for a hybrid electric vehicle," *Journal of Automobile Engineering*, vol. 216, no. 11, pp. 855–864, 2002.

[3] G. Sovran and D. Blaser, "Quantifying the potential impacts of regenerative braking on a vehicle's tractive fuel consumption for the U.S., European, and Japanese driving schedules," SAE Paper 2006-01-0664, 2006.

[4] Y. Gao, "Electronic braking system of EV and HEV integration of regenerative braking, automatic braking force control and ABS," SAE Paper 2001-01-2478, 2001.

[5] K. Muta, M. Yamazaki, and J. Tokieda, "Develop-ment of new-generation hybrid system THS II—drastic improvement of power performance and fuel economy," SAE Paper 2004-01-0064, 2004.

[6] F. Wyczalk, "Regenerative braking concepts for electric vehicle-a primer," SAE Paper 920648, 1992.

[7] H. Yeo, C. Song, C. Kim, and H. Kim, "Hardware in the loop simulation of hybrid vehicle for optimal engine operation by CVT ratio control," *International Journal of Automotive Technology*, vol. 5, no. 3, pp. 201–208, 2004.

[8] Y. Luo, P. Li, D. Jin, and K. Li, "A study on regenerative braking strategy based on optimal control theory," *Automotive Engineering*, vol. 28, no. 4, pp. 356–360, 2006.

[9] G. Yin, N. Chen, and P. Li, "Improving handling stability performance of four-wheel steering vehicle via μ-synthesis robust control," *IEEE Transactions on Vehicular Technology*, vol. 56, no. 5, pp. 2432–2439, 2007.

[10] O. Tur, O. Ustun, and R. N. Tuncay, "An introduction to regenerative braking of electric vehicles as anti-lock braking system," in *Proceedings of the IEEE Intelligent Vehicles Symposium (IV '07)*, pp. 944–948, Istanbul, Turkey, June 2007.

[11] T. Okano, S. Sakai, T. Uchida, and Y. Hori, "Braking performance improvement for hybrid electric vehicle based on electric motor's quick torque response," in *Proceedings of the 19th International Battery Hybrid and Fuel Cell Electric Vehicle Symposium*, pp. 1285–1296, Busan, Republic of Korea, October 2002.

[12] J.-H. Pu, C.-L. Yin, and J.-W. Zhang, "Fuzzy torque control strategy for parallel hybrid electric vehicles," *International Journal of Automotive Technology*, vol. 6, no. 5, pp. 529–536, 2005.

[13] D. Peng, Y. Zhang, C.-L. Yin, and J.-W. Zhang, "Combined control of a regenerative braking and antilock braking system for hybrid electric vehicles," *International Journal of Automotive Technology*, vol. 9, no. 6, pp. 749–757, 2008.

[14] L. Wu and D. W. C. Ho, "Sliding mode control of singular stochastic hybrid systems," *Automatica*, vol. 46, no. 4, pp. 779–783, 2010.

[15] R. Yang, H. Gao, and P. Shi, "Delay-dependent robust H_∞ control for uncertain stochastic time-delay systems," *International Journal of Robust and Nonlinear Control*, vol. 20, no. 16, pp. 1852–1865, 2010.

[16] H. B. Pacejka and E. Bakker, "Magic formula tyre model," *Vehicle System Dynamics*, vol. 21, no. 1, pp. 1–18, 1992.

[17] J. Li, J. W. Zhang, and F. Yu, "An investigation into fuzzy controller for anti-lock braking system based on road autonomous identification," SAE Paper 2001-01-0599, 2001.

[18] L. Wu and W. X. Zheng, "Passivity-based sliding mode control of uncertain singular time-delay systems," *Automatica*, vol. 45, no. 9, pp. 2120–2127, 2009.